THE ASTROPHYSICAL JOURNAL, 178:25–44, 1972 November 15

THE REDSHIFT-DISTANCE RELATION. III. PHOTOMETRY AND THE HUBBLE DIAGRAM FOR RADIO SOURCES AND THE POSSIBLE TURN-ON TIME FOR QSOs

ALLAN SANDAGE
Hale Observatories, Carnegie Institution of Washington, California Institute of Technology
Received 1972 May 8

ABSTRACT

UBV photometry is given for 59 radio galaxies, and is summarized for 103 radio and 25 radio-quiet quasars. The Hubble diagram for the radio galaxies is similar to that for first-ranked cluster galaxies, but is displaced faintward by 0.3 mag in the mean.

If $H_0 = 50$ km s^{-1} Mpc^{-1}, then $\langle M_v \rangle = -22.98$ with $\sigma = 0.49$ mag for radio galaxies, and $\langle M_v \rangle = -23.26$ with $\sigma = 0.32$ mag for first-ranked cluster galaxies. Radio galaxies can be as bright as the brightest E galaxies in clusters, but their luminosity distribution is asymmetric, reaching fainter limits.

If the mass-to-light ratio is 30 in visual solar units, a galaxy must have a mass greater than $10^{12}\ \mathfrak{M}_\odot$ to be a strong radio source. First-ranked cluster galaxies and the brightest radio galaxies have an upper limit to their mass that is of order $10^{13}\ \mathfrak{M}_\odot$.

The Hubble diagram for quasars is scattered, but no quasars lie to the right (fainter) of the radio galaxy distribution. This can be understood if a quasar consists of a normal strong radio galaxy upon which a nonthermal component is superposed which has a wide intrinsic dispersion (factor of ~ 50) to its optical luminosity. Quasars are then at their Hubble distance.

The apparent cutoff in quasar redshifts near $z = 2.8$ is examined for selection effects that could produce it artificially. If the cutoff is real, it may be the time of the birth of the first quasars, although the suggested redshift is unexpectedly small. At $z = 3$ in a $q_0 = +1$ universe, the look-back time is 89 percent of the Friedmann age. Assessment of the observational selection effects shows that none are positively established that would produce the cutoff artificially. Special observations to test its reality are straightforward and can be made with existing ground-based telescopes, but they have not yet been done.

Previously unreported photometry for 22 quasars is listed in an appendix.

I. INTRODUCTION

The first optical identifications of radio galaxies in the early 1960's showed that such galaxies are, in general, elliptical systems. Some are in clusters, some in groups, but many are isolated in the field. Excluding the exceptional cases such as Per A, Vir A, Cyg A, and Cen A, they are of normal optical appearance.

By 1960, redshifts for some of the identified galaxies were known from earlier studies (cf. references in Maltby, Matthews, and Moffet 1963). Bolton (1960) combined his estimates of apparent magnitude with the available redshifts to show that the galaxies then identified were intrinsically bright optically. How general was this early result?

To obtain additional data, a photometric program was begun in 1964 to measure magnitudes and colors of identified radio galaxies in the 3CR Cambridge catalog (Bennett 1962). The first observing list contained galaxies for which Schmidt (1965) and others had measured the redshifts. The program was later expanded to include most of the identified 3CR galaxies that either had redshifts measured later by other observers (references set out in notes to table 2), or for which redshifts would eventually be obtained.

After the discovery of quasars and the later heavy effort to identify them, the photometric program was extended to include all classes of 3CR identifications. Most of the photometric data on QSOs were published as they were obtained. Discussions of the Hubble diagram for quasars were given by several authors who used part of the QSO data, but the difficulty with such discussions is that they have usually been made in isolation from the data for radio galaxies (e.g., Hoyle and Burbidge 1966; Longair and Scheuer 1967).

The purposes of this paper are (1) to list the new photometric data for radio galaxies and obtain therefrom the (V_c, z) number pairs for the Hubble diagram for such systems (§ II); (2) to determine the optical luminosity function for radio galaxies in the sample and to compare this with the luminosities of first-ranked cluster galaxies; (3) to discuss the Hubble diagram for quasars and radio galaxies together (§ IV); (4) to relate the results to the question of quasar distances (§ V); and (5) to discuss the evidence and the selection effects for an upper limit to quasar redshifts near $z \simeq 3$, and the implications that such a cutoff, if real, would have for the problem of finding the edge of the quasar distribution in space and time (§ VI).

II. PHOTOMETRIC DATA FOR RADIO GALAXIES

The photometry was done with the Mount Wilson and Palomar 60-, 100-, and 200-inch (152-, 254-, and 508-cm) reflectors using 1P21 photomultipliers and filters made from 2.8 mm of Corning 9863 for U, 0.7 mm of Schott BG12 + 2 mm of Schott GG13 for B, and 2.8 mm of Schott GG11 for V. No red-leak corrections were applied, as tests showed that none were required at the 0.01 mag level in the color ranges encountered.

The data are listed in table 1. Column (2) gives the telescope used; observations made by others are indicated in this column. Column (3) gives the diameter of the measuring aperture in arc seconds; chart numbers are given in column (7) with a listing at the end of the table: numbers or letters in parentheses in this column indicate the galaxy identification on the particular chart. The final column gives particular circumstances of the galaxy or of the photometry. Dumbbells, or contamination by other galaxies and stars, are noted. Seyfert and N galaxies are noted.

The magnitudes listed for 3C 295 are newly measured and replace the old value given by Minkowski (1960) as estimated from Baum's unpublished results.

The errors of the photometry should generally be less than $\sim \pm 0.05$ mag for all colors and magnitudes.

The data in table 1 were corrected for aperture effect by the precepts of Paper I (Sandage 1972*a*). The corrected data, designated V_{26} and B_{26}, are listed in table 2 (cols. [7] and [8]), together with the redshift in column (4). Column (5) refers to the observer responsible for the redshift, as explained in the notes. Corrections for K-dimming and absorption were made by using the precepts of Paper II (Sandage 1972*b*). The adopted absorptions are in columns (9) and (10). The V_c and B_c magnitudes, corrected for aperture, absorption, and K effects, are given in columns (11) and (12); the corrected color in column (13), the absolute magnitude calculated from the redshift using a Hubble constant of $H_0 = 50$ km s^{-1} Mpc^{-1} and $q_0 = +1$ is in column (14), and the log of the proper radio luminosity (in ergs s^{-1}) as discussed in § VI is listed in column (15). In the "Remarks," column (16), information such as NGC or Abell cluster number, or classification data (Db for Dumbbell) is given. No magnitudes are listed for the N galaxies because a special discussion is required to separate the quasarlike component from the galaxy light in the combined (measured) intensity (Paper IV).

TABLE 1

PHOTOELECTRIC DATA FOR RADIO GALAXIES

Object	Tel	Aperture	V	B-V	U-B	Chart	Remarks
3C15	200	7|6	16.29	1.14	....	11	Brightest member of small group
		12.2	15.94	1.19	....		
		12.2	15.89	1.17	....		
		18.8	15.70	1.13	....		
		30.6	15.51	1.09	....		
17	200	7|6	18.42	0.81	....	1	Isolated. N?
		12.2	18.15	1.03	....		
		12.2	18.23	1.05	....		
26	200	12.2	18.10	0.97	....	Matthews unpub.	Isolated
		12.2	18.18	1.06	....		
28	200	12.2	17.87	1.50	....	1	Brightest member of rich cluster, A115.
		12.2	17.79	1.39	....		
		18.8	17.62	1.33	....		
		18.8	17.47	1.45	....		
29	200	12.2	15.05	1.06	....	1	Outlying member of rich Abell cluster 119?
		18.8	14.68	1.08	0.52		
		30.6	14.41	1.05	....		
31	60P	68.8	12.53	1.18:	....	1	NGC 383, SO_3. In small group of HMS, table XI.
33	200	12.2	15.85	1.14	....	2	Isolated
		18.8	15.63	1.16	....		
		30.6	15.45	1.14	....		
		48.3	15.27	1.01	....		
40	100	35.2	12.97	1.03	....	2,3,4	NGC545 3C40 is NGC545 and is brightest
		64.0	12.09	1.01	....		NGC545 / NGC547 member of a cluster, A194.
		112	11.85	1.04	....		
		35.2	12.97	1.04	....		NGC547 N2 of Griffin is NGC545 which is the radio source. N3 of
		35.2	13.31	1.03	....		
		64.0	12.87	1.02	....		NGC541 Griffin is NGC547.
		112	12.58	0.96	....		N1 of Griffin is NGC541.
66	100	11.2	14.81	0.90	....	2,3,(1)	N1 On outskirts of
		20.0	13.86	1.08	....		N1+Star cluster A347. If
		35.2	13.40	0.86	....		Star alone a member it is the brightest.
71	60	17.2	10.56	0.80	0.11	3	NGC 1068
	100	6.4	11.61	0.88	-0.01		
	100	20.0	10.56	0.80	0.11		
	60H	Total	8.91	0.82	....		
75	100	64.0	13.29	1.16	....	2,3,(1,2)	N1+N2 Dumbell, Δmag=0.3
		112	13.06	1.21	....		N1+N2 In small cluster A400.
76.1	200	12.2	15.88	1.13	0.63	1	Isolated
		18.8	15.60	1.14	0.53		
		30.6	15.44	1.15	....		
78	100	35.2	13.41	1.20	....	2	NGC1218, isolated
		64.0	13.04	1.16	....		
		112	12.79	1.19	....		
79	200	7.6	18.75	0.79	-0.27	1,5	Isolated. N? Varies?
		12.2	18.49	0.93	....		
		12.2	18.62	0.88	....		
84	60	24.6	12.91	0.72	0.04	3	NGC1275. Per A.
		24.6	12.96	0.70	0.07		Brightest member
		41.6	12.53	0.76	0.09		of Perseus cluster
		41.6	12.58	0.73	0.12		or A426.
		69.2	12.18	0.81	0.16		
		69.2	12.28	0.75	0.11		
M03-31	100P Sersic	202 Total	9.14 8.9	0.91 1.0	....	8	Fornax A=NGC1316. Brightest in Fornax Cl.
88	100	35.2	14.45	1.12	....	1	Isolated
		64.0	14.07	1.14	....		
89	200	12.2	17.06	1.55	....	1,5	In a small group no red-
		18.8	16.76	1.50	....		This is the radio shift
		30.6	16.56	1.50	....		source yet
89b	200	12.2	17.36	1.53	....		Galaxy 32" NW
		18.8	17.06	1.46	....		of 3C89.
		30.6	16.86	1.45	....		
3C98	100	35.2	14.80	1.28	....	2,3(1)	N alone
		64.0	14.14	1.05	....		N+star
		11.2	14.96	0.99	0.72		star alone
109	200	7.6	18.05	0.93	-0.15	1.5	Isolated N Sept. 10/67
		7.6	18.02	1.00	....		Nov. 3, 67 Varies
		12.2	17.76	0.89	-0.08		Feb. 14, 65
		12.2	18.01	0.91	-0.29		Nov. 2, 67
		12.2	18.05	0.95	....		Nov. 24, 67
120	200						Isolated, N or Sy Varies
		7.6	14.19	0.46	-0.76		Sept. 10, 67
		7.6	14.21	0.46	-0.79		Sept. 11, 67
		7.6	14.23	0.57	-0.78		Nov 1, 67
		7.6	14.32	0.52	-0.83		Nov 24, 67
		12.2	14.11	0.49	-0.78		Sept. 11, 67
		12.2	14.14	0.60	-0.75		Nov 1, 67
		12.2	14.21	0.59	-0.81		Nov 24, 67
		18.8	14.02	0.52	-0.75		Sept. 11, 67
		18.8	14.07	0.63	-0.74		Nov 1, 67
		18.8	14.11	0.62	-0.78		Nov 24, 67
		30.6	13.92	0.57	-0.74		Sept. 11, 67
135	200	12.2	17.36	1.23	....	1	In small gr? N?
		12.2	17.40	1.31	0.33		Varies?
		12.2	17.35	1.42	0.60		
		18.8	17.18	1.23	....		
		18.8	17.26	(1.33)	....		
171	200	12.2	18.93	0.95	....	1,3,5	Isolated. N
		12.2	18.85	0.66	....		
192	200	12.2	16.15	1.14	0.39	1,5	In small group.
		18.8	15.92	1.16	0.39		
192b	200	18.8	16.17	1.20	0.80	1	70"W, 13"N of 3C192
197.1	200	12.2	17.50	1.28	....	1	In small no red-
		18.8	17.32	1.23	....		cluster shift yet
198	200	12.2	17.33	0.71	-0.25	1	Maybe in a small
		18.8	17.09	0.83	-0.18		group
212	200	7.6	19.06	0.90	-0.30	1	Isolated? N
219	200	12.2	17.49	1.50	....	2	Has companion In 18"8; measure- rich
		18.8	17.10	1.57	....		ment may be cluster contaminated.
223	200	12.2	17.41	1.26	....	1,5	In a group
		18.8	17.16:	1.24	....		
223.1	200	12.2	16.75	1.24	0.15	1	Isolated? May be in
		18.8	16.57	1.25	0.28:		small, faint group
		30.6	16.54	1.23	....		
227	200	12.2	16.44	0.95	-0.39	1	N.
		18.8	16.33	0.98	-0.25:		
231	60H	Total	8.39	0.91	....	5	M82. Exploding galaxy.
234	200	12.2	17.27	0.94	-0.41		N. In group of compact galaxyies.
236	200	18.8	16.23	1.24	0.33	1	Isolated? In a faint
		30.6	16.00	1.13	....		group?
264	200	12.2	14.15	1.05	0.46	1	NGC3862
		18.8	13.86	1.03	0.49		
		30.6	13.58	1.02	0.49		
		48.3	13.28	1.03	0.51		
264a	200	18.8	14.67	1.05	0.59	1	Companion galaxy
		30.6	14.53	1.01	0.60		55"N, 18"W of 3C264
270	De Vauc	Total	10.4	1.0	....	2	NGC4261
272.1	Holmberg	Total	9.36	0.95	....	3	NGC4374, M84
274	Holmberg	Total	8.74	0.98	....	...	NGC4486, M87
277.3	200	12.2	16.50	1.28	0.47	3(1)	Coma A
		18.8	16.25	1.19	0.38		

(continued)

TABLE 1 -continued

Object	Tel	Aperture	V	B-V	U-B	Chart	Remarks
278	100	20.0	12.95	1.01	0.67	2,3(1)	NGC4782. Dumbell
		35.2	12.41	0.96	0.67		This is the radio
		64.0	11.97	0.99	0.58		source.
278a	100	20.0	13.14	0.96	0.63	2,3(2)	NGC4783. Companion
		35.2	12.67	0.95	0.54		to 3C278
		64.0	12.18	0.94	0.52		
M13-42	Holmberg	Total	6.98	0.99	....	3,8	Cen A, NGC5128
3C285	200	12.2	16.59	1.02	0.28	1	Brightest member of
		18.8	16.35	0.99	0.24		group.
		30.6	16.09	1.04	....		
287.1	200	7.6	18.27	0.92	-0.15	1	N. Isolated
293	200	18.8	15.10	1.00	0.31	6	Isolated
		30.6	14.67	0.98	....		
		48.3	14.44	0.99	....		
295	200	7.6	19.76	1.46	....	7	More details are in the
		12.2	19.56	1.38	....		Addendum to Table 1 of
							Paper II.
296	200	12.2	13.70	1.03	....	1	IC5532. Has companion
		18.8	13.27	1.08	....		35" S of source
		30.6	12.92	1.03	-0.58		
		48.3	12.63	1.01	0.59		
305	200	12.2	14.66	0.96	0.39	1,5	Isolated
		18.8	14.30	0.94	0.33		
		18.8	14.34	0.88	....		
		30.6	14.05	0.88	0.32		
310#1	200	12.2	16.17	1.16	0.51	3(1)	Dumbell, N. W. component
		12.2	16.11	1.16	....		
		18.8	15.78:	0.97:	0.78		
		18.8	15.65	1.16	....		
310#2	200	12.2	16.31	1.15	0.55	3(2)	Dumbell. S.E. component
		12.2	16.12:	....	....		
		18.8	15.85	1.14	0.44		
		18.8	15.75	1.14	....		
Near 310	200	12.2	16.33	1.23	0.53	3	Companion 55" E of #1
		18.8	16.09	1.17	0.47		
315	200	18.8	16.49	1.19	0.44	3(1,2)	Dumbell. Photometry
		18.8	16.49	1.22	....		includes both
		30.6	16.27	1.14	....		components. $\Delta m = 0^m.5$
317#2	200	30.6	14.06	1.07	0.40	3(2),8	In cluster A2052.
		48.3	13.62	1.06	....		
317#3	200	30.6	14.72	1.02	0.55	3(3),8	
327	200	12.2	16.31	1.39	0.28	3(1)	
		18.8	16.08	1.35	0.30		
338	O'Dell	Total	12.47	0.83	....	8,9	NGC6166. Brightest member
							of cluster A2199.
348	200	18.8	17.05	1.46	....	2b,3(1,2)	Her A.
		30.6	16.80	1.40	....	10	
353	200	12.2	16.56	1.51	....	3(1)	Isolated
		18.8	16.22	1.59	0.95		
		30.6	15.89	1.41	....		
371	200	7.6	14.90	0.68	-0.38	1	N galaxy in group
		7.6	14.81	0.72	-0.35		Varies!1st line June 20, 66
		7.6	14.30	0.61	-0.44		2nd line June 21,66. 3rd
							line Aug. 11, 67.
		7.6	14.22	0.55	-0.48		Sept. 8, 67
		7.6	14.22	0.58	-0.48		Sept. 10, 67
		7.6	14.26	0.59	-0.48		Sept. 11, 67
		7.6	14.20	0.57	-0.48		Sept. 12, 67
		18.8	14.30	0.61	-0.38		Oct. 27, 67
		12.2	14.46	0.63	-0.42		Oct. 31, 67
		12.2	14.50	0.65	-0.34		Nov. 2, 67
Near 371	200	12.2	16.11	0.99	....		Bright group member SW
		18.8	15.88	1.01	....		of 3C371.
381	200	12.2	17.52	1.40	....	1	Brightest in small group.
382	200	12.2	15.39	1.11	-0.10	1	Isolated
386	200	18.8	14.24	1.17	.....	3(1)	
388	200	18.8	15.56	1.35	....	3(1,2),5	Photometry includes
		30.6	15.24	1.32	....		secondary galaxy 8"
		48.3	14.99	1.31	....		distant in envelope
							$\Delta m \sim 2$ mag.
390.3	200	7.6	15.49	0.80	-0.59	1,Parker	N. Has companion
		12.2	15.40	0.81	-0.59		
		12.2	15.38	0.82	-0.56		
Near 390.3	200	12.2	16.48	1.16	.....	5(a)	Galaxy 27" E, 61" N
		18.8	15.98	1.03	Clouds?		of 390.3
403	200	12.2	15.81	1.29	0.47	1	Includes 17 mag star.
		18.8	15.48	1.24	.....		Includes two 17 mag.
							stars.
Star near 403	200	7.6	14.00	1.45	1.65	1	Bright star 16" SE of
							403
405	200	18.8	15.72	1.44	.....	3(1,2)	Cyg A. In a moderately
		18.8	15.79	1.53	.....	8	rich cluster
		30.6	15.25	1.37	.....		
		30.6	15.35	1.47	.....		
Near 405	200	12.2	17.35	1.37	.....	8	Galaxy 34" W, 10" N
		12.2	17.33	1.48	.....		3C405
Star near 405	200	12.2	14.27	1.24	0.93	8	Star 27"E of 3C405.
433	200	18.8	15.74	1.59	0.59	6	Double. $\Delta m = 0.0$ mag.
							Photometry includes
							both components.
436	200	12.2	(18.64)	(1.25)	.....	1,5	Photometry uncertain
442	100	20.0	14.67	1.08	0.57	3(2)	NGC7237 In an extended cluster
		35.2	14.20	1.09	0.52		
		64.0	13.74	0.92	....		
Near 442	100	20.0	14.24	1.03	0.51	3(1)	NGC7236
		35.2	13.99	1.04	0.52		
444	200	12.2	17.36	1.26	....	6	In a cluster. No
		18.8	16.75	1.30	....	Von Hoerner	redshift yet.
445	100	11.2	15.72	1.18	.....	3(1)	N isolated
		11.2	15.78	1.20	.....		
	200	12.2	15.84	1.17	-0.15		
		18.8	15.76	1.15	-0.19		
449	100	24.0	14.19	0.87	.....	1	Brightest in
		37.6	14.02	0.88	.....		small group
452	200	12.2	16.56	1.04	.....	1,5	Probably in a
							cluster
455	100	20.0	14.71	1.00	0.46	6	Isolated
		35.2	14.47	0.97	....		
456	200	12.2	18.70	0.95	....	1	Slight uncertainty
							of 0.5 mag in gain
							step
459	200	12.2	17.54	0.86	-0.30	1,5	N.
		12.2	17.55	0.86	-0.30		
		12.2	17.56	0.85	-0.48		
M23-112	200	18.8	15.83	1.06	....	Matthews	May be member of
		30.6	15.52	0.97	....	unpublished	cluster A2638.
		30.6	15.53	1.11	....		
465	200	12.2	14.43	1.16	....	8	N1 N2 is galaxy
		12.2	15.08	1.11	....		N2 in envelope of
		48.3	13.19	1.12	....		N1+N2 N1. $\Delta m = 0.7$ mag
		72.4	12.94	1.09	....		N1+N2 In cluster
							A2634. The
							source is
							NGC7720.

REFERENCES FOR FINDING CHARTS TO TABLE 1.—(1) Wyndham 1966; (2) Maltby *et al.* 1963; (3) Griffin 1963; (4) Zwicky and Humason 1964; (5) Longair 1965; (6) Wyndham 1965; (7) Minkowski 1960; (8) Matthews *et al.* 1964; (9) Minkowski 1961; (10) Greenstein 1962; (11) Hazard 1965; (12) Kinman 1968.

TABLE 2

SUMMARY OF PHOTOMETRIC DATA FOR 69 RADIO SOURCES

Source	l^{II}	b^{II}	z	z ref	log cz	V_{26}	B_{26}	A_V	A_B	V_C	B_C	B_C-V_C	M_{VC}	$\log L_R$	Remarks
(1)	(2)	(3)	(4)	(5)	(6)	(7)	(8)	(9)	(10)	(11)	(12)	(13)	H=50	H=50	(16)
3C15	115	-64	0.0733	EMB	4.342	15.34	16.46	0.00	0.00	15.22	16.09	0.87	-22.99	42.98	In group
17	115	-65	0.2201	MS	4.820	18.02	19.04	0.00	0.00	17.56	17.97	0.41	-23.04	43.92	
26	125	-67	0.2106	MS	4.801	17.94	18.96	0.00	0.00	17.51	17.89	0.38	-23.00	43.46	
28	124	-37	0.1959	MS	4.769	17.54	19.00	0.12	0.16	17.05	17.84	0.79	-23.30	43.48	Cl A115
29	127	-64	0.0450	AS2	4.127	14.07	15.13	0.00	0.00	14.00	14.90	0.90	-23.14	42.61	
31	127	-30	0.0170	HMS	3.706	12.14	13.30	0.21	0.27	11.90	12.95	1.05	-23.13	41.70	NGC383
33	129	-49	0.0600	MS	4.255	15.19	16.30	0.01	0.01	15.08	15.98	0.90	-22.70	43.14	
40	142	-63	0.0180	RM,M^3	3.732	12.28	13.32	0.00	0.00	12.25	13.23	0.98	-22.91	41.83	Cl A194
66	140	-17	0.0215	RM,M^3	3.810	12.90	13.86	0.24	0.32	12.63	13.44	0.81	-22.92	41.87	(Cl A347)
71	172	-52	0.0038	HMS	3.053	8.91	9.73	0.00	0.00	8.91	9.73	0.82	-22.86	40.25	N1068Sy
75*	170	-45	0.0241	RM,M^3	3.859	13.62	14.80	0.04	0.06	13.54	14.62	1.08	-22.26	42.02	Db
76.1	163	-36	0.0328	AS2	3.993	14.86	15.98	0.13	0.17	14.68	15.64	0.96	-21.78	42.01	
78	175	-45	0.0289	MS	3.938	12.84	14.02	0.04	0.06	12.75	13.82	1.07	-23.44	42.21	N1218
79	164	-35	0.2561	MS	4.886	N	N	0.14	0.19	N	N	N		43.98	
84	151	-13	0.0181	HMS	3.735	11.87	12.62	0.30	0.40	11.54	12.13	0.59	-23.64	42.23	N1275Sy
Fornax A	240	-57	0.0051	HMS	3.184	8.9	9.9	0.00	0.00	8.90	9.90	1.00	-23.74	41.78	N1316
88	181	-42	0.0302	MS	3.957	13.95	15.06	0.07	0.10	13.83	14.81	0.98	-22.46	42.17	
98	180	-31	0.0306	MS	3.963	(14.45)	(15.66)	0.19	0.25	(14.21)	15.25	1.04	-22.10	42.46	
109	182	-28	0.3060	RL	4.963	N	N	0.23	0.31	N	N	N		44.07	
120	190	-27	0.0333	EMB	4.000	13.78	14.35	0.25	0.33	13.48	13.85	0.37	-23.02	42.40	Sy
135	200	-21	0.1270	AS2	4.581	17.00	18.24	0.37	0.50	16.42	17.09	0.67	-22.98	43.21	
171	162	22	0.2387	MS	4.855	N	N	0.35	0.47	N	N	N		43.88	
192	198	26	0.0596	AS	4.252	15.46	16.60	0.26	0.35	15.10	15.95	0.85	-22.66	42.71	
198	218	23	0.0809	MS	4.385	16.78	17.56	0.32	0.44	16.33	16.70	0.37	-22.09	42.80	
219	174	45	0.1745	MS	4.719	17.22	18.74	0.04	0.06	16.87	17.78	0.91	-23.22	43.91	Anon Cl.
223	188	49	0.1367	AS	4.613	17.06	18.30	0.01	0.01	16.83	17.59	0.76	-22.74	43.19	
223.1	183	49	0.1075	AS	4.509	(16.36)	(17.60)	0.01	0.01	(16.18)	17.04	0.86	-22.86	42.74	
227	229	42	0.0855	AS2	4.409	N	N	0.07	0.10	N	N	N		43.22	
231	141	40	.....	HMS	.....	8.39	9.30	0.09	0.12	8.30	9.18	0.88	M82	39.40	M82
234	200	53	0.1846	MS	4.743	N	N	0.00	0.00	N	N	N		43.80	In group
236	190	54	0.0988	AS2	4.472	15.97	17.14	0.00	0.00	15.81	16.64	0.83	-23.05	43.09	
264	236	73	0.0206	MS	3.791	12.74	13.80	0.00	0.00	12.71	13.70	0.99	-22.74	41.89	N3862
270	282	67	0.0070	HMS	3.321	10.4	11.4	0.00	0.00	10.4	11.40	1.00	-22.70	41.49	N4261
272.1	278	74	0.0029	HMS	2.944	9.36	10.31	0.00	0.00	9.36	10.31	0.95	-21.86	40.39	N4374
274	284	75	0.0041	HMS	3.086	8.74	9.72	0.00	0.00	8.74	9.72	0.98	-23.19	41.97	M87
277.3	72	89	0.0857	MS	4.410	15.94	17.20	0.00	0.00	15.80	16.76	0.96	-22.75	42.80	Coma A
278*	273	50	0.0143	JLG	3.633	11.46	12.44	0.00	0.00	11.44	12.37	0.93	-23.22	41.65	Db
Cen A	309	19	0.0016	HMS	.....	6.98	7.97	0.43	0.58	6.55	7.39	0.84	(-20.95)	41.01	N5128
3C285	103	73	0.0797	AS2	4.379	15.99	17.02	0.00	0.00	15.86	16.61	0.75	-22.54	42.63	
287.1	326	63	0.2156	AS	4.811	N	N	0.00	0.00	N	N	N		43.65	
293	54	76	0.0454	AS	4.134	14.32	15.29	0.00	0.00	14.25	15.06	0.81	-22.92	42.51	
295	98	61	0.461	RM,B	5.141	20.11	21.53	0.00	0.00	18.63	19.63	1.00	-23.57	45.09	
296	354	62	0.0237	AS	3.852	12.21	13.24	0.00	0.00	12.17	13.12	0.95	-23.59	41.90	IC5533
305	103	49	0.0416	AS	4.096	13.74	14.60	0.01	0.01	13.66	14.38	0.72	-23.32	42.27	
310*	39	60	0.0543	MS	4.212	15.24	16.38	0.00	0.00	15.15	16.10	0.95	-22.41	42.94	Db
315*	39	58	0.1086	MS	4.513	16.80	17.96	0.00	0.00	16.62	17.40	0.78	-22.44	43.15	Db
317	9	50	0.0351	MS	4.022	13.50	14.54	0.00	0.00	13.44	14.36	0.92	-23.17	42.48	
327	12	38	0.1041	MS	4.495	15.88	17.22	0.11	0.15	15.60	16.54	0.94	-23.38	43.48	
338	63	44	0.0303	RM	3.958	12.63	13.46	0.05	0.08	12.53	13.21	0.68	-23.76	42.28	
348	23	29	0.1540	JLG	4.665	16.90	18.42	0.22†	0.29	16.42	17.34	0.92	-23.40	44.68	Her A
353	21	20	0.0307	MS	3.964	15.36	16.86	1.26†	1.68†	14.05	15.02	0.97	-22.27	43.18	
371	100	29	0.0508	AS	4.183	N	N	0.22	0.29	N	N	N		42.35	
381	76	23	0.1614	AS2	4.685	17.24	18.64	0.07†	0.10†	16.89	17.71	0.82	-23.04	43.47	
382	61	17	0.0586	MS	4.245	14.66	15.76	0.00†	0.00†	14.56	15.46	0.90	-23.16	42.73	
388*	75	20	0.0917	MS	4.439	15.32	16.62	0.21	0.28	14.96	15.87	0.91	-23.74	43.17	Db
390.3	112	27	0.0569	AS	4.232	N	N	0.25	0.33	N	N	N		42.98	
403	42	-12	0.059	RL	4.248	15.42	16.68	0.37	0.50	14.96	15.88	0.92	-22.78	42.80	
405	76	6	0.0570	RM	4.233	(15.14)	(16.59)	0.90†	1.20†	(14.15)	(15.10)	0.95	-23.52	45.32	Cyg A
433*	75	-18	0.1025	MS	4.488	16.24	17.82	0.93†	1.24†	15.14	16.05	0.91	-23.80	43.58	Db
436	80	-19	0.2154	MS	4.810	18.18	19.66	0.43†	0.58†	17.31	17.99	0.68	-23.24	43.71	
442*	75	-34	0.0270	JLG	3.908	(13.66)	(14.66)	0.16	0.20	(13.46)	(14.33)	0.87	-22.58	41.92	N7237
445	62	-47	0.0568	MS	4.231	N	N	0.03	0.04	N	N	N		42.77	
449	95	-16	0.0181	AS2	3.735	13.20	14.07	0.48	0.66	12.69	13.32	0.63	-22.48	41.56	
452	98	-17	0.0820	MS	4.391	16.00	17.04	0.45†	0.60†	15.41	16.01	0.60	-23.04	43.37	
455	85	-41	0.0331	AS2	3.997	14.00	14.98	0.09	0.11	13.86	14.70	0.84	-22.62	42.04	
456	86	-46	0.2337	MS	4.846	(18.54)	(19.49)	0.04	0.05	18.00	18.26	0.26	-22.73	43.71	
459	83	-51	0.2205	MS	4.821	N	N	0.00	0.00	N	N	N		43.86	
MSH23-112	66	-64	0.0825	MS	4.394	15.46	16.52	0.00	0.00	15.33	16.10	0.77	-23.14	42.69	
465	104	-33	0.0301	MS	3.956	13.29	14.41	0.17	0.22	13.07	14.04	0.97	-23.21	42.35	N7720

*Dumbells. Photometry has been reduced to the brightest components. Result is usually uncertain by a few tenths of a magnitude.
†E(B-V) from colors.

REDSHIFT REFERENCES TO TABLE 2.—MS, Schmidt 1965; M³, Maltby, Matthews, and Moffet 1963; JLG, Greenstein 1961, 1962; RM, Minkowski 1961; EMB, Burbidge 1967; RL, Roger Lynds, private communication; HMS, Humason, Mayall, and Sandage 1956; AS, Sandage 1966*a*; AS2, Sandage 1967*b*.

III. THE HUBBLE DIAGRAM AND THE DISTRIBUTION OF M_V FOR RADIO GALAXIES IN THE SAMPLE

a) Discussion

The $[V_c, \log z]$ pairs for the 59 non-N galaxies in table 2, and the 10 radio galaxies listed in table 3 of Paper II (data by Westerlund and Wall), are plotted in the Hubble diagram of figure 1. A line of slope 5 is shown, fitted in zero-point to pass through the mean of the data. Its equation is

$$V_c = 5 \log cz - 6.46 . \quad (1)$$

Most of the galaxies in table 2 have the optical appearance of normal ellipticals. Figure 2 is a histogram of corrected colors $B_c - V_c$ for the 59 radio galaxies of table 2, compared with the nonradio galaxies from table 2 and 3 of Paper II. Figure 2 shows that the bulk of the radio galaxies have $0.7 < B_c - V_c < 1.1$, as for normal ellipticals. Only 11 galaxies (18 percent of the sample) are bluer than this, and most of these have prominent emission lines that affect the color.

Comparison of equation (1) here with equation (4) of Paper II shows that the present sample of radio galaxies is fainter than first-ranked cluster galaxies by $\Delta M_V \simeq 0.30$ mag. A detailed comparison is shown in figure 3, which is the distribution of M_V for the present sample (table 2 here and table 3 of Paper II), compared with that for first-ranked cluster galaxies (Paper II). The mean absolute magnitude for the radio galaxies in the sample is $\langle M_{Vc} \rangle = -22.98$ with $\sigma = 0.49$ mag while that for first-ranked galaxies is $\langle M_{Vc} \rangle = -23.26$ with $\sigma = 0.316$ mag, adopting $H_0 = 50$ km s^{-1} Mpc^{-1}. Figure 3, with its asymmetrical distribution for radio galaxies, shows that galaxies which are themselves fainter than the first-ranked in clusters can also be strong (i.e., $L_r \gtrsim 10^{40}$ ergs s^{-1}) radio sources; nevertheless, such galaxies must be near the bright end of the luminosity function. Well-known radio galaxies that are not first-ranked cluster members would include NGC 1265 and IC 310 in the Perseus cluster, and M87 in Virgo.

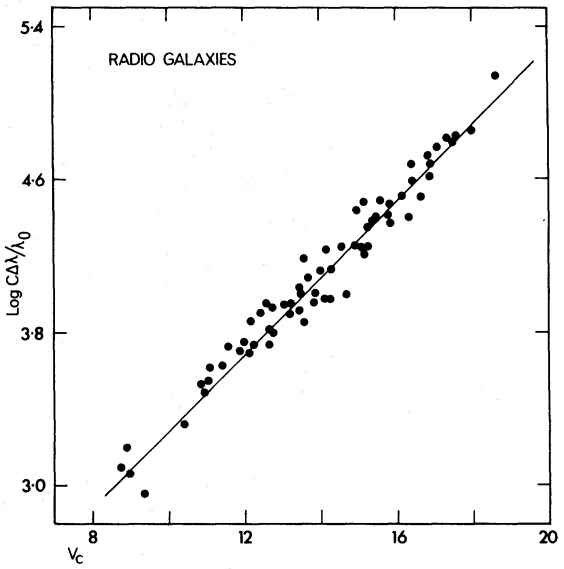

FIG. 1.—The Hubble diagram for 59 radio galaxies of table 2, together with 10 additional galaxies from table 3 of Paper II. No N galaxies are included. The line is equation (1) of the text, and is 0.3 mag fainter than drawn for first-ranked cluster galaxies in figs. 2–4 of Paper II.

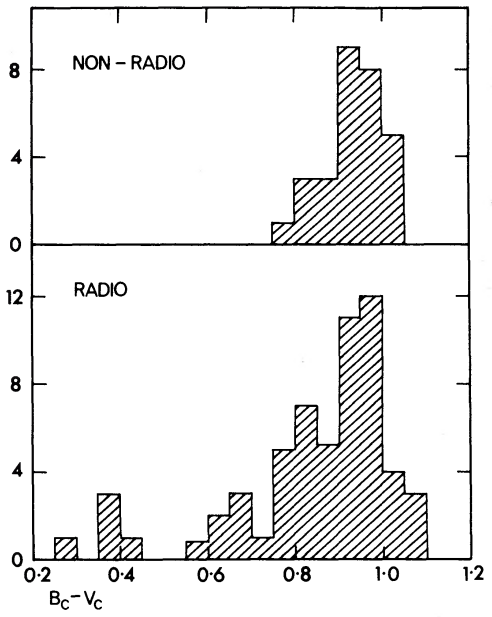

FIG. 2

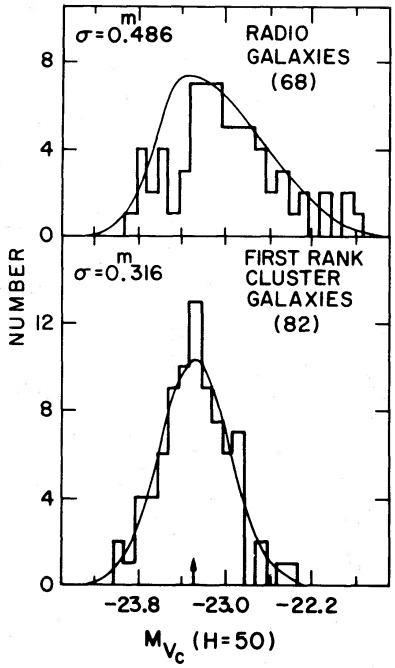

FIG. 3

FIG. 2.—Distribution of corrected $B_c - V_c$ colors for radio galaxies of table 2, compared with 29 nonradio cluster E and S0's from table 2 of Paper II.

FIG. 3.—Optical luminosity functions for radio galaxies (table 2), and first-ranked cluster galaxies (Paper II). The absolute magnitudes are based on $H_0 = 50$ km s^{-1} Mpc^{-1}. The bright edge of the solid curve in the upper panel is the same as the lower, but renormalized. The faint edge is a Gaussian with $\sigma(M_v) = 0.486$ and $\langle M_v \rangle = -22.98$. The mean of each distribution is: (*upper*) $\langle M_v \rangle = -22.98$, (*lower*) $\langle M_v \rangle = -23.26$.

Figure 3 does show, however, that there is a restriction on how faint a galaxy can be to be a strong radio source. Systems that are fainter than ~ 2.5 mag from the brightest, or 1.5 mag fainter than the mean, do not generate radio energy at a rate faster than $L_R \simeq 10^{40}$ ergs s^{-1}. The present results are consistent with the findings of Rogstad and Ekers (1969) who made a special survey of known E and S0 galaxies for radio emission. All detected galaxies of these classes that have $L_R \gtrsim 10^{40}$ ergs s^{-1} were of high optical absolute magnitude.

Figure 3 shows an additional significant feature. The bright end of the luminosity function for radio galaxies and for first-ranked cluster members is the same. The point is illustrated by noting that the solid line on the left of each distribution in figure 3 has been normalized to the same Gaussian and the fit is good for both distributions.

b) Conclusions

1. Galaxies that are strong radio sources are intrinsically bright optically. They can be as bright as the brightest E galaxies in clusters, but their luminosity distribution is asymmetrical, reaching fainter limits than first-ranked cluster galaxies.

2. It appears that a necessary condition for a galaxy to be a strong radio source is that it be brighter than the lower cutoff luminosity in figure 3 (viz., $M_V \simeq -21.8$ if $H_0 = 50$ km s^{-1} Mpc^{-1}). If the mass-to-visual light ratio is 30 in solar units, this gives a mass of $\mathfrak{M}_{\min} \gtrsim 10^{12}\,\mathfrak{M}_\odot$. The upper mass limit for galaxies in our present sample (figure 3) is obtained from M_V (max) $= -24.0$, or $\mathfrak{M}_{\max} \simeq 10^{13}\,\mathfrak{M}_\odot$, if $\mathfrak{M}/L_V = 30$.

TABLE 3

SUMMARY OF REDSHIFTS, PHOTOMETRY, AND RADIO POWER FOR QSO'S

Source (1)	l^{II} (2)	b^{II} (3)	Z (4)	Z source (5)	log CZ (6)	m-M H=50 (7)	V (8)	B (9)	B-V (10)	U-B (11)	M_V H=50	log L_R H=50
						3C Sources						
3C2	99	-61	1.037	7	5.493	43.96	19.35	20.14	+0.79	-0.96	-24.61	44.97
9	112	-47	2.012	1	5.781	45.40	18.21	18.44	+0.23	-0.74	-27.19	45.51
47	137	-41	0.425	2	5.106	42.03	18.1	18.2	+0.05	-0.65	-23.9	44.41
48	134	-29	0.367	3	5.042	41.71	16.2	16.62	+0.42	-0.58	-25.51	44.75
57	173	-67	0.670	29	5.303	43.01	16.40	16.54	+0.14	-0.73	-26.61	43.01
94	197	-43	0.962		5.460	43.80	16.49	16.93	+0.44	-0.68	-27.31	43.80
95	205	-46	0.614		5.265	42.83	16.24	16.35	+0.11	-0.65	-26.59	42.83
138	187	-11	0.759	4	5.357	43.29	17.9	18.13	+0.23	-0.38	-25.39	45.03
147	162	+10	0.545	2	5.214	42.57	16.9	17.25	+0.35	-0.59	-25.67	45.20
175	205	+10	0.768	7	5.362	43.31	16.60	17.05	+0.45	-0.50	-26.71	44.76
181	204	+15	1.382	5	5.627	44.59	18.92	19.35	+0.43	-1.02	-25.67	45.19
186	182	+26	1.063	4	5.504	44.02	17.60	18.05	+0.45	-0.71	-26.42	45.04
191	212	+21	1.946	6,22	5.766	45.33	18.4	18.65	+0.25	-0.84	-26.93	45.42
196	171	+33	0.871	4	5.417	43.59	17.6	18.20	+0.60	-0.43	-25.99	45.48
204	150	+36	1.112	5	5.524	44.12	18.21	18.76	+0.55	-0.99	-25.91	44.36
207	214	+30	0.683	7	5.312	43.06	18.15	18.58	+0.43	-0.42	-24.91	44.49
208	214	+33	1.110	5,8	5.524	44.12	17.42	17.76	+0.34	-1.00	-26.70	45.07
215	212	+37	0.411	4	5.091	41.96	18.27	18.48	+0.21	-0.66	-23.68	43.96
232	194	+52	0.534	19	5.205	42.52	15.78	15.88	+0.10	-0.68	-26.75	44.00
245	233	+56	1.029	1,9	5.490	43.95	17.25	17.70	+0.45	-0.83	-26.70	44.88
246	260	+43	0.344	30	5.014	41.57	16.79	16.85	+0.06	-0.49	-24.78	41.57
249.1	130	+38	0.311	5,15,23	4.970	41.35	15.72	15.70	-0.02	-0.77	-25.63	43.84
254	173	+66	0.734	1	5.343	43.21	17.98	18.13	+0.15	-0.49	-25.23	44.78
261	200	+73	0.614	4,20	5.265	42.83	18.24	18.48	+0.24	-0.56	-24.59	44.20
263	134	+50	0.652	15,23	5.291	42.96	16.32	16.50	+0.18	-0.56	-26.64	44.52
268.4	147	+71	1.400	19	5.623	44.62	18.42	19.00	+0.58	-0.69	-26.20	45.05
270.1	167	+81	1.519	5	5.657	44.79	18.61	18.80	+0.19	-0.61	-26.18	45.14
273	290	+64	0.158	10	4.676	39.88	12.8	13.0	+0.21	-0.85	-27.08	44.35
275.1	293	+79	0.557	4	5.223	42.61	19.00	19.23	+0.23	-0.43	-23.61	44.43
277.1	123	+60	0.320	5,23	4.982	41.41	17.93	17.76	-0.17	-0.78	-23.48	43.82
279	305	+58	0.536	9,11	5.206	42.53	17.75	18.01	+0.26	-0.56	-24.78	44.63
280.1	115	+77	1.659	4	5.697	44.98	19.44	19.31	-0.13	-0.70	-25.54	45.17
281	314	+69	0.599	23	5.255	42.77	17.02	17.15	+0.13	-0.59	-25.75	42.77
286	57	+81	0.846	9,12	5.404	43.52	17.30	17.52	+0.22	-0.84	-26.22	45.30
287	23	+81	1.054	1	5.500	44.00	17.67	18.30	+0.63	-0.65	-26.33	45.15
288.1	112	+56	0.961	19	5.460	43.80	18.12	18.51	+0.39	-0.82	-25.68	44.76
298	352	+61	1.439	4	5.635	44.68	16.79	17.12	+0.33	-0.70	-27.88	45.72
309.1	111	+41	0.903	7,20	5.433	43.66	16.78	17.24	+0.46	-0.77	-26.88	45.11
323.1	34	+49	0.264	19	4.899	40.99	16.69	16.80	+0.11	-0.85	-24.30	43.73
334	33	+41	0.555	9,13	5.222	42.61	16.41	16.53	+0.12	-0.59	-26.20	44.31
336	41	+42	0.927	4	5.444	43.72	17.47	17.91	+0.44	-0.79	-26.25	44.83
345	63	+41	0.594	9,13	5.251	42.75	16.0	16.29	+0.29	-0.50	-26.75	44.65
351	90	+36	0.371	9	5.046	41.73	15.28	15.41	+0.13	-0.75	-26.45	44.10
380	77	+24	0.691	9,13	5.317	43.08	16.81	17.05	+0.24	-0.59	-26.27	45.28
432	68	-23	1.804	5	5.734	45.17	17.96	18.18	+0.22	-0.79	-27.21	45.28
446	59	-49	1.403	5,13	5.625	44.62	18.39	18.83	+0.44	-0.90	-26.23	45.36
454	87	-36	1.756	5	5.722	45.11	18.40	18.52	+0.12	-0.95	-26.71	45.21
454.3	86	-39	0.860	7,21	5.412	43.56	16.10	16.57	+0.47	-0.66	-27.46	45.29
						4C Sources						
4C-5.93	59	-50	1.981	7	5.774	45.37	17.70	18.45	+0.75	-0.71	-27.67	44.83
-05.6	152	-66	0.308	7	4.966	41.33	18.25	18.29	+0.04	-0.81	-23.08	43.16
-03.7	172	-57	2.064	7	5.792	45.46	16.96	17.03	+0.07	-0.82	-28.50	44.86
-00.6	127	-63	0.717	7	5.332	43.16	17.33	17.53	+0.20	-0.70	-25.83	44.48
1.4	147	-59	0.261	7,21,25	4.894	40.97	17.07	17.12	+0.05	-1.02	-23.90	43.26
4.6	174	-56	1.439	23,25	5.636	44.67	16.46	16.61	+0.15	-0.89	-28.22	44.48
5.34	217	+19	2.877	28	5.936	46.18	18.16	18.53	+0.37	-0.04	-28.0	45.02
15.1	107	-45	0.450	7	5.130	42.15	16.40	16.51	+0.11	-0.70	-25.75	43.83
20.33	18	+67	0.871	4	5.417	43.59	17.65	18.09	+0.44	-0.69	-25.94	44.60
21.35	257	+81	0.435	7,20	5.116	42.08	17.50	17.56	+0.06	-0.69	-24.58	43.88
29.50	51	+35	1.927		5.762	45.31	19.14	19.29	+0.15	-0.86	-26.17	45.06
29.68	102	-30	1.015	5,7,25	5.484	43.92	17.30	17.95	+0.65	-0.87	-26.62	44.61
31.38	193	+77	1.557	20	5.669	44.85	18.96	19.33	+0.37	-0.65	-25.89	45.02
37.24	185	+35	0.914	7	5.438	43.69	18.11	18.53	+0.42	-0.81	-25.58	44.65
39.25	184	+46	0.698	4,20	5.321	43.10	17.86	17.92	+0.06	-0.31	-25.24	44.52
						OTHERS						
MSH03-19	206	-47	0.614	5	5.265	42.83	16.24	16.35	+0.11	-0.65	-26.59	44.59
13-011	323	+55	0.625	20	5.274	42.87	17.68	17.82	+0.14	-0.66	-25.19	44.50
14-121	345	+41	0.942	5,17	5.450	43.75	17.37	17.81	+0.44	-0.76	-26.38	44.98
CTA102	77	-38	1.038	1	5.493	43.97	17.32	17.74	+0.42	-0.79	-26.65	45.33
						PKS						
0106+01	131	-61	2.107	8	5.801	45.50	18.39	18.54	+0.15	-0.70	-27.11	45.13
0119-04	142	-65	1.955	25	5.768	45.34	17.03	17.49	+0.46	-0.82	-28.31	44.94
0122-00	140	-62	1.070	7	5.506	44.03	16.70	16.98	+0.28	-0.75	-27.33	44.54
0159-11	173	-67	0.68	26	5.310	43.05	16.40	16.54	+0.14	-0.73	-26.65	44.55
0229+13	157	-43	2.067	25	5.793	45.46	17.71	17.96	+0.25	-0.73	-27.75	44.73
0237-23	209	-65	2.223	31	5.824	45.62	16.63	16.78	+0.15	-0.61	-28.99	45.28
0350-07	196	-43	0.962	7	5.461	43.80	16.49	16.93	+0.44	-0.68	-27.31	44.90
0403-13	206	-42	0.571	7	5.233	42.67	17.09	17.37	+0.28	-0.57	-25.58	44.50
0405-12	204	-42	0.574	25	5.236	42.68	14.79	14.97	+0.18	-0.60	-27.89	.....
0736+01	218	+11	0.191	7	4.758	40.29	16.47	16.90	+0.43	-0.77	-23.82	43.44

TABLE 3 -continued

Source	l^{II}	b^{II}	Z	Z Source	log CZ	m-M	V	B	B-V	U-B	M_V	Log L_R
(1)	(2)	(3)	(4)	(5)	(6)	H=50	(8)	(9)	(10)	(11)	H=50	H=50
0812+02	221	+19	0.402	25	5.081	41.90	.....	.....	.....	.....	.....	44.03
0837-12	237	+17	0.200	25	4.778	40.39	15.76	15.78	+0.02	-0.85	-24.63	43.40
0859-14	242	+21	1.327	20	5.600	44.50	16.59	16.79	+0.20	-0.85	-27.91	45.04
0922+14	216	+41	0.900	4,15,23	5.431	43.66	17.96	18.50	+0.54	-0.52	-25.70	44.35
A00952+17	216	+48	1.471	25	5.645	44.72	17.23	17.31	+0.08	-0.74	-27.49	(44.9)
0957+00	239	+41	0.908	4,15,23	5.435	43.68	17.57	18.04	+0.47	-0.71	-26.11	44.34
1049-09	260	+43	0.344	25	5.014	41.57	16.79	16.85	+0.06	-0.49	-24.78	43.79
1116+12	242	+64	2.118	5,18	5.802	45.52	19.25	19.39	+0.14	-0.76	-26.26	45.34
1127-14	275	+44	1.187	20	5.552	44.26	16.90	17.17	+0.27	-0.70	-27.36	45.29
1136-13	277	+46	0.554	25	5.221	42.60	.....	.....	.....	.....	.....	44.60
1148-00	272	+59	1.982	20	5.774	45.37	17.60	17.77	+0.17	-0.97	-27.77	45.28
1217+02	284	+63	0.240	4,15,23	4.857	40.79	16.53	16.51	-0.02	-0.87	-24.26	43.18
1229-02	292	+60	0.388	25	5.066	41.83	16.75	17.23	+0.48	-0.66	-25.08	43.91
1233-24	299	+38	0.355		5.027	41.64	17.19	17.55	+0.36	-0.58	-24.45	43.97
1252+11	306	+75	0.870	5,9,23	5.416	43.58	16.64	16.99	+0.35	-0.75	-26.94	44.39
1327-21	296	+41	0.528	20	5.199	42.50	16.74	16.84	+0.10	-0.54	-25.76	44.23
1354+19	8	+72	0.720	20	5.334	43.17	16.02	16.20	+0.18	-0.55	-27.15	44.50
1454-06	350	+45	1.249	20	5.574	44.37	18.03	18.39	+0.36	-0.82	-26.34	44.79
1510-08	353	+40	0.361	20	5.035	41.67	16.52	16.69	+0.17	-0.74	-25.15	44.12
2115-30	16	-43	0.98	26	5.468	43.84	16.39	17.09	+0.70	-0.47	-27.45	44.77
2135-14	40	-43	0.202	27	4.778	40.39	15.53	15.63	+0.10	-0.83	-24.86	43.62
2146-13	42	-45	1.800	7	5.732	45.16	.....	.....	.....	.....	.....	45.21
2216-03	60	-46	0.901	7	5.431	43.66	16.38	16.93	+0.55	-0.62	-27.28	.....
2251+11	83	-42	0.323	25	4.986	41.43	15.80	16.01	+0.21	-0.84	-25.63	43.70
2344+09	97	-50	0.677	25	5.308	43.04	15.92	16.15	+0.23	-0.61	-27.12	44.33
2354+14	103	-46	1.810	25	5.735	45.17	18.18	18.32	+0.14	-0.90	-26.99	45.22
PHL938	127	-60	1.93	14	5.762	45.31	17.16	17.48	+0.32	-0.88	-28.15	
957	127	-50	2.70	33	5.908	46.04	16.57	16.97	+0.40	-0.28	-29.47	
1027	142	-58	0.363	32	5.037	41.68	17.04	17.01	-0.03	-0.77	-24.64	
1127	146	-55	1.990	24	5.776	45.38	18.29	18.43	+0.14	-0.83	-27.09	
1186	146	-51	0.270	24,32	4.908	41.04	17.4	17.4	-0.02	-0.81	-23.64	
1194	147	-51	0.298	24	4.951	41.26	17.50	17.43	-0.07	-0.85	-23.76	
3375	140	-54	0.390	32	5.068	41.84	18.02	18.31	+0.29	-0.51	-23.82	
3424	142	-56	1.847	24	5.744	45.22	18.25	18.44	+0.19	-0.90	-26.97	
3632	145	-54	1.479	32	5.647	44.74	18.15	18.28	+0.13	-0.75	-26.58	
BS13	44	+79	1.287	32	5.587	44.43	17.94	18.41	+0.47	-0.71	-26.49	
						RADIO QUIET						
Ton256	43	+45	0.131	16	4.593	39.46	15.41	16.06	+0.65	-0.78	-24.06	N gal.
BS01	124	+80	1.241	27	5.571	44.35	16.98	17.29	+0.31	-0.78	-27.37	
2	125	+82	(0.186)	27	(4.747)	40.23	18.64	18.92	+0.28	-0.98	(-21.59)	
6	104	+83	1.956	27	5.768	45.34	17.87	17.92	+0.05	-1.01	-27.47	
11	95	+80	2.084	27	5.796	45.48	18.41	18.47	+0.06	-0.85	-27.07	
B46	126	+82	0.271	27	4.910	41.05	17.83	18.19	+0.36	-0.87	-23.22	Fuzzy, N?
114	116	+82	(0.221)	27	(4.822)	40.61	17.92	18.00	+0.08	-0.90	(-22.69)	
154	112	+82	(0.183)	27	(4.740)	40.20	18.56	18.88	+0.32	-0.70	(-21.64)	
189	112	+80	2.075	27	5.794	45.47	19.22	19.19	-0.03	-0.83	-26.25	
194	112	+82	1.864	27	5.748	45.24	17.96	18.36	+0.40	-0.76	-27.28	
201	110	+82	1.375	27	5.615	44.58	16.79	17.05	+0.26	-0.82	-27.79	
234	108	+81	0.060	27	4.255	37.78	17.52	18.38	+0.86	-0.43	-20.26	Sharp lines
264	96	+85	0.095	27	4.455	38.77	16.89	17.47	+0.58	-0.65	-21.88	N
312	106	+80	(0.450)	27	(5.130)	(42.15)	19.08	19.22	+0.14	-0.67	(-23.07)	
340	101	+82	0.184	27	4.742	40.21	16.97	17.38	+0.41	-0.74	-23.24	

REDSHIFT REFERENCES TO TABLE 3

1. Schmidt, M.S. 1965, Ap. J., 141, 1295.
2. Schmidt, M.S., and Matthews, T. A. 1964, Ap. J., 139, 781.
3. Greenstein, J. L., and Matthews, T. A. 1963, Nature, 197, 1041.
4. Lynds, C. R., Hill, S. J., Heere, K., and Stockton, A. N. 1966, Ap. J., 144, 1244.
5. Schmidt, M. S. 1966, Ap. J., 144, 443.
6. Burbidge, E. M., Lynds, C. R., and Burbidge, G. R. 1966, Ap. J., 144, 447.
7. Lynds, C. R. private communication, 1967, Ap. J., 147, 837.
8. Burbidge, E. M. 1966, Ap. J., 143, 612.
9. Lynds, C. R., Stockton, A. N., and Livingston, W. C. 1965, Ap. J., 142, 1667.
10. Schmidt, M. S. 1963, Nature, 197, 1040.
11. Burbidge, E. M., and Rosenburg, F. D. 1965, Ap. J., 142, 1673.
12. Oke, J. B. 1965, Ap. J., 142, 810.
13. Burbidge, E. M. 1965, Ap. J., 142, 1674.
14. Kinman, T. 1966, Ap. J., 144, 1232.
15. Rubin, V. C., and Ford, W. K. 1966, Ap. J., 145, 357.
16. Sandage, A. R. 1965, Ap. J., 141, 1560.
17. Burbidge, E. M. 1965, Ap. J., 142, 1291.
18. Lynds, C. R., and Stockton, A. N. 1966, Ap. J., 144, 446.
19. Schmidt, M. S. 1966 Private letter, Yearbook Carnegie Inst. 1965-66.
20. Burbidge, E. M., and Kinman, T. D. 1966, Ap. J., 145, 654.
21. Schmidt, M. S. 1966, Private Communication.
22. Stockton, A. N., and Lynds, C. R. 1966, Ap. J., 144, 451.
23. Hiltner, W. A., Cowley, A. P., Schild, R. E. 1966, Pub. A. S. P., 78, 464.
24. Sandage, A., and Luyten, W. J. 1967, Ap. J., 148, 767.
25. Kinman, T. D., and Burbidge, E. M., Ap. J. Letters, 148, L59.
26. Searle, L., and Bolton, J. G. 1968, Ap. J. Letters, 154, L101.
27. Braccesi, A., Lynds, R., and Sandage, A. 1968, Ap. J. Letters, 152, L105.
28. Lynds, R., and Wills, D. 1970, Nature, 206, 532.
29. Schmidt, M. 1968, Ap. J., 151, 393.
30. Kinman, T. D., and Burbidge, E. M. 1967, Ap. J. Letters, 148, L59.
31. Arp, H. C., Bolton, J. G., and Kinman, T. D., 1967, Ap. J., 147, 840.
32. Burbidge, E. M. 1968, Ap. J., 154, L109.
33. Lowrance, J.L. et. al., 1971, Ap. J., 171, 233.

IV. QUASARS

a) The Data

Listed in table 3 are data taken from a file catalog kept current at the Hale Observatories until 1970. The table is divided into sections according to the original source catalog. The 3C, 4C, and Parkes listings make up the bulk of the radio sources. The radio-quiet list contains objects that have been previously discussed in the literature.

The redshift in column (4) is from the literature, referenced by a code number in column (5) whose key is at the end of the table. Column (7) gives the distance modulus calculated from the redshift value in column (6) using $H_0 = 50$ km s^{-1} Mpc^{-1} and $q_0 = +1$. The photometry in columns (8)–(10) is either from the literature (mostly *Ap. J.* from 1963 to 1968), or from the Appendix here. Most of the photometry was obtained with the 200-inch Palomar reflector in the present program, although some entries are due to Kinman, Lynds, and others. Column (12) gives the absolute V-magnitude found from column (7) and (8). Column (13) is the log of the absolute radio power as discussed in § VI.

No K-corrections have been applied to the data, because these are much smaller than the intrinsic scatter of the absolute luminosities (Sandage 1966*b*). No correction for galactic absorption was applied for the same reason. The measuring aperture was usually 7″.6 in diameter, although occasionally it was increased to 12″.2 in bad seeing.

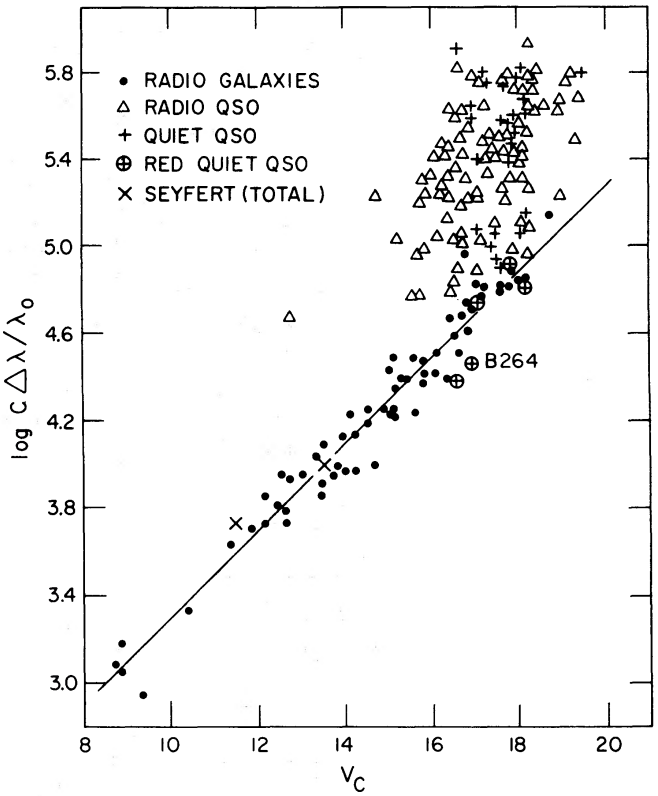

FIG. 4.—The Hubble diagram for radio quasars from table 3 (*triangles*), radio-quiet quasars from table 3 plus unpublished data (*vertical crosses*), radio galaxies from table 2 of this paper and table 3 of Paper II (*dots*), Seyfert galaxies from Sandage (1967*c*), and radio-quiet quasars that are redder than the normal $B - V = f(z)$ relation caused by the underlying galaxy affecting the colors, as in N galaxies (*crossed circles*). No corrections have been applied to the quasar magnitudes. Corrections to galaxy magnitudes are for K-dimming, aperture effect, and galactic absorption.

For quasars, the nonthermal component usually dominates the light of the system and no aperture correction should be needed with these hole sizes because the quasar component is always optically unresolved, and light from the larger underlying galaxy is almost always negligible compared with the total.

b) *The Hubble Diagram*

Figure 4 is the Hubble diagram from these data in V-magnitudes. Radio quasars are shown as triangles, radio-quiet quasars as vertical crosses, and radio galaxies as dots. The data are from table 2 for the galaxies, and table 3 for the quasars, as supplemented by additional data on radio-quiet quasars from a current program (Sandage and Schmidt, unpublished). The Seyfert galaxy data are from a previous study (Sandage 1967*c*).[1]

There are two significant features of figure 4. (*A*) No quasars lie to the right of the galaxy distribution. This appears significant to me, even though the overlap region in redshift ($0.16 \leq z \leq 0.5$) is small. (*B*) Redshifts for quasars in the present sample are less than $z \simeq 3$, and the distribution ends abruptly there, shown by the well-defined upper envelope at $\log cz \simeq 5.9$. I shall argue that the first of these has bearing on the controversy of quasar distances, and that the second, if real, tells us something about the matter-horizon of the Universe in space and time.

V. INTERPRETATION OF THE QUASAR DISTRIBUTION IN THE HUBBLE DIAGRAM

That there are no quasars to the right of the galaxy distribution would follow naturally from a model where various amounts of nonthermal radiation (the QSO component) are added to an underlying galaxy. The total light of the system will be greater than its parts, and if the underlying galaxy, being a radio source, must come from the M_V (radio) distribution of figure 3, the composite object cannot then be fainter than the faintest radio galaxy taken alone. (We take the point of view that it is required that a massive galaxy be present to produce [host?] the strong radio source; i.e., the quasar component seen optically has itself no part in the radio phenomenon.)

The point concerning luminosities is made more explicitly in figure 5, which is the distribution of absolute magnitudes for the present sample (Paper II, and here with $H_0 = 50$ and $q_0 = +1$). The upper two panels are slight variations of figure 3. The third panel shows that the 103 radio QSOs of table 3 are all brighter than the faintest radio galaxy.

The restriction of being to the left of the galaxy line need not necessarily apply to *radio-quiet* quasars because we have no evidence that the optical luminosity of the underlying galaxy need be high, since such galaxies are themselves radio-quiet and do not need to be larger than that critical mass that is required for radio sources (§ III). The lower panel of figure 5 shows that a few radio-quiet quasars are indeed fainter than their radio counterparts. But the bulk of the sample is, in fact, similar in their M_V distribution to the radio QSOs, and the fainter objects are either incipient N galaxies or are too red (R) for their redshift (Sandage 1966*b*, fig. 1) as noted by R or N in the diagram.[2]

[1] The most striking feature of the diagram is the large scatter of the quasars. This need have no significance other than a large spread in absolute luminosity.

[2] The lower two panels of figure 5 cannot be interpreted as the luminosity function of QSOs because several selection effects have not been accounted for there. The most severe are (1) the observer's cutoff in the redshift programs near $V \simeq 19.5$ (evident in fig. 4), and (2) the effect that radio QSOs are selected from radio catalogs that have fixed lower flux limits. This means that the absolute radio power which a QSO has to have to be catalogued must be higher, the higher the redshift, and this progressively diminishes the number of QSOs as z increases by a factor that follows directly from the radio luminosity function. If there is any correlation between optical and radio luminosity, this could affect the distribution in M_V at different z values.

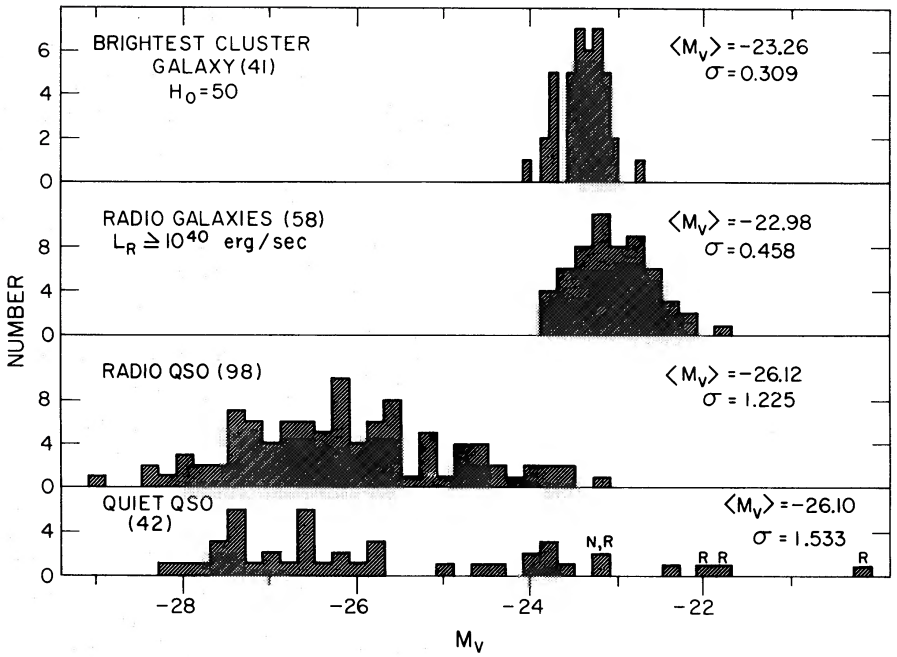

FIG. 5.—Distribution of absolute luminosity for four groups of objects calculated using $H_0 = 50$ km s^{-1} Mpc^{-1}. Symbols N and R in lower panel denote N-galaxy characteristics or redder colors than normal for a quasar at the given redshift.

Exploratory calculations have been made of the efficiency of contamination of galaxy light by various amounts of a QSO component (Sandage 1971, § IV, tables 4, 5, and 6). These show that adding larger proportions of QSO light to the mix causes the $B - V$ and $U - B$ colors to change from nuclear M31–like colors, through colors appropriate to N galaxies (Sandage 1967*a*), into the quasar region of the two-color diagram. By the time the mix contains equal proportions of galaxy and QSO light at λ(proper) = 5500 Å, the composite color is $B - V = 0.28$, $U - B = -0.77$ (at $z = 0$) and most vestiges of the underlying galaxy have disappeared.

Quite generally, the calculations show that by the time the magnitude difference between the quasar and the galaxy line in figure 4 reaches $\Delta V \simeq 1$ mag, signs of the underlying galaxy in the *UBV* colors and in the optical image (detection of a galaxy disk) will be marginal.

The calculations further show (Sandage 1971, table 5 and fig. 10) that there is a twilight zone when $\Delta V \lesssim 1$ mag, where evidence of the underlying galaxy is present either in the colors, or by directly seeing it on plates. The results of Kristian's (1972) photographic survey of intrinsically faint quasars near the galaxy line in the Hubble diagram are consistent with these ideas, as are the properties of N galaxies.

That N systems are intermediate cases where the quasar contamination is too small to obliterate the galaxy, as in QSOs, yet large enough to give a more abnormal system than Seyferts is shown by Arp's (1970) photographic study of 3C 371, where the underlying normal galaxy is clearly visible on long-exposure photographs.

From these ideas it follows naturally that N galaxies (where the contamination ratio is $\lesssim 0.2$) will not deviate far from the Hubble line for radio galaxies in the Hubble diagram (Sandage 1967*a*, fig. 2, and Paper IV of this series), but that quasars should do so by amounts that depend on the strength of the nonthermal component. The pre-

sent data are then consistent with the view that quasars are at the Hubble distance. If they were not, then the lack of quasars on the faintward side of the galaxy distribution in the Hubble diagram would not be understood.

The conclusion is the same as that which follows from the surface-brightness correlations of Heeschen (1966), the angular-diameter measurements of multiple-component quasars by Hogg (1969), Legg (1970), and Miley (1971), the general similarity of the separate distributions of linear separations of the multiple radio components of radio galaxies and of quasars (assumed to be at the Hubble distance) discussed by Ryle (1968, especially fig. 9) and studied more recently by Mackay (1971), the evidence by Gunn (1971), and the direct discovery of underlying galaxies to several quasars by Kristian (1972).[3]

VI. AN UPPER LIMIT TO QUASAR REDSHIFTS AND THE EDGE OF THE WORLD

a) Selection Effects

i) *Discussion*

The second interesting feature of figure 4 is the apparent redshift cutoff at log $cz \simeq 5.9$ ($z \simeq 2.8$) for quasars in the present sample. Is it real or is it caused by selection effects?

One observational restriction is that the redshifts have been observed for very few quasar candidates fainter than $V \simeq 19.5$. However, this alone is not sufficient to make an artificial redshift cutoff, as can be seen from the construction in figure 6.

Here the vertical line at $B = 19.5$ represents the present observer-imposed limit. This is extended upward until it intersects the upper envelope to the QSO distribution (taken here as a line of slope 5) at log $cz \simeq 6.4$, or $z \simeq 8$. The envelope line is made to pass through the intrinsically brightest quasar (optically) PKS 0237−23, and is the brightness limit in absolute luminosity of the observed quasars in this sample. The hatched area between these two lines is, then, the region which is not denied the observer if quasars do indeed exist with $z > 2.8$, provided that there are no other selection effects.

But there are two others.

1. Triangles in figure 6 are objects identified from *radio* catalogs, and the problem mentioned in n. 2 exists. That is, if there is an upper limit to absolute radio luminosity, and if we use a radio-source catalog with a fixed lower limit to the apparent flux density, then there will be a *maximum* redshift beyond which the intrinsically brightest source will be fainter than the catalog limit. As long as quasar identifications were made from the 3C catalog alone, where sources fainter than 9 flux units (178 MHz) are not listed, the intrinsically most luminous sources at $L_R \simeq 4 \times 10^{45}$ ergs s^{-1} are at the catalog limit for redshifts of $z \simeq 2.5$ (cf. Sandage 1966*c*, fig. 5 and item *B* on page 33). No objects with large redshifts are in the 3C. Consequently, an artificial cutoff would be produced in figure 6 near $z \simeq 2.5$, which is close to the observed value.

Strong as this argument was for 3C sources, it cannot be the explanation of the cutoff in figure 4 because redshifts have now been measured for radio quasars identified from fainter catalogs.

Figure 7 shows the nature of the current observational restriction of this kind. Plotted is the log of the radio power as ordinate, and redshift (*top*) or distance

[3] Against this multiple evidence must be put the observation by Arp (1971) of Markarian 205 which may possibly be connected to NGC 4319 by a luminous filament, but yet has a different redshift. Proof that the connection is real in three dimensions does not exist, small as the contrary probability may be. That the filament itself is real may also be open to question (Lynds and Millikan 1972).

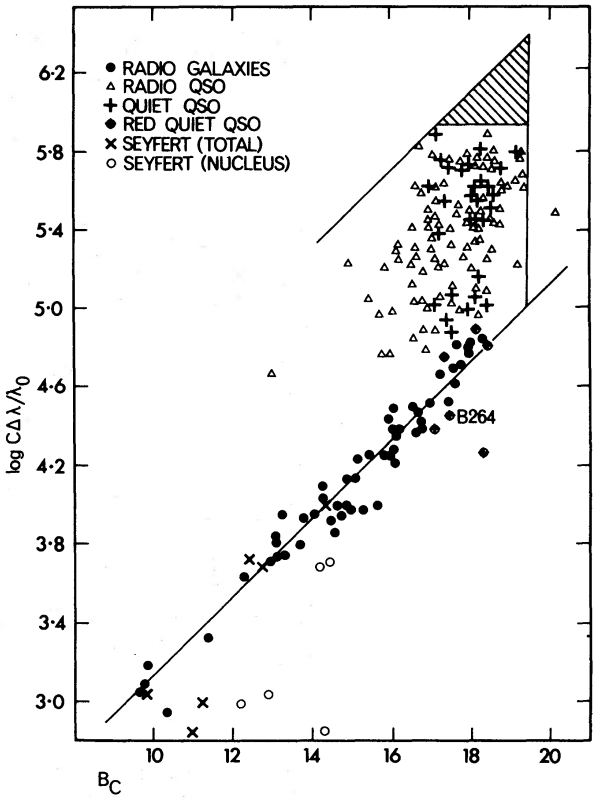

FIG. 6.—Same as figure 4 but for B_c. The vertical line at $B_c \simeq 19.5$ intersects the upper-envelope Hubble line of slope 5 at $z \simeq 8$.The hatched area should contain quasars if they exist, except for the radio apparent flux selection effect on the triangles, and the optical $U - B$ guillotine effect on the radio-quiet QSO for redshifts larger than 2. That these may not be important and that the apparent cutoff in redshifts may be real is discussed in the text.

modulus (*bottom*) as abscissa, calculated from $m - M = 5 \log cz + 16.50$, which assumes $H_0 = 50$ km s^{-1} Mpc^{-1}.

The radio power was found for each source listed in tables 2 and 3 by integration of the radio spectrum over proper frequencies from 10^7 to 10^{10} Hz and assuming $q_0 = +1$, as follows. If the radio spectrum has the form

$$S = A\nu^{-n} \text{ W m}^{-2} \text{ Hz}^{-1}, \tag{2}$$

then the energy contained between *observed* frequencies ν_1 and ν_2 is

$$l = A \int_{\nu_1}^{\nu_2} \nu^{-n} d\nu \text{ W m}^{-2}. \tag{3}$$

A K-correction must be applied to change l from that given by equation (3) to what would have been observed in the rest frame of the source. Both the bandwidth term and the effect of shifting the spectrum through the frequency-window of the detector are involved, and, by the standard theory, the K-corrected flux l' is related to the observed flux l by

$$l' = (1 + z)^{1-n} l. \tag{4}$$

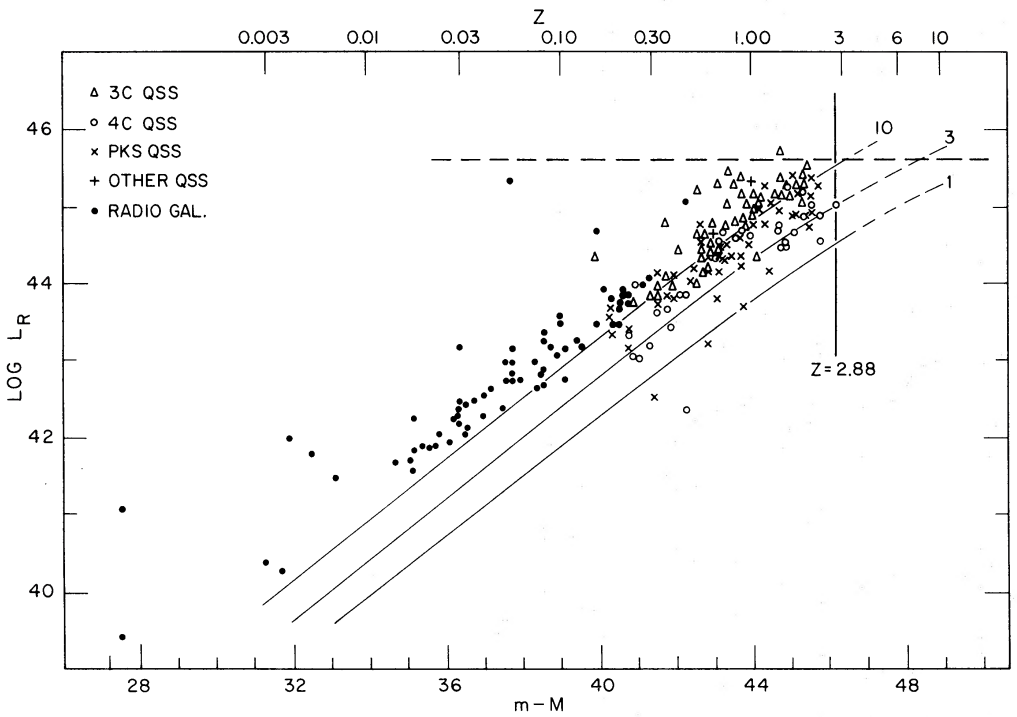

FIG. 7.—The radio power plotted against redshift for radio galaxies from table 2 and quasars from tables 3 and 4. Quasars are *triangles* if from the 3C catalog, *open circles* if 4C, *crosses* if Parkes, and *vertical crosses* if others. The radio galaxies are *dots*. Lines of apparent flux densities are shown at 10, 3, and 1 flux units at 178 MHz. No part of the area between the f = 3. f.u. line and the upper-envelope line at 4×10^{45} ergs s^{-1} should be denied the observer by selection effects if the 4C catalog is used. The lack of redshifts larger than $z \simeq 2.8$ in the area to the right of the vertical line suggests that such redshifts do not occur.

Hence, the intrinsic radio power between *proper* frequencies ν_1 and ν_2 is, for $q_0 = +1$,

$$L_R = 4\pi c^2 z^2 l' H_0^{-2}, \tag{5}$$

which, with $H_0 = 50$ km s^{-1} Mpc^{-1}, gives

$$L_R = 4.3 \times 10^{44}(1 + z)^{1-n} z^2 l \quad \text{ergs s}^{-1}. \tag{6}$$

For many sources in tables 2 and 3, the l values between 10^7 and 10^{10} Hz are listed by Kellermann (1964, final column of his table 2), and these were used directly. For sources not listed there, data in the catalog of Howard *et al.* (1965) permitted transformation to the system of equation (6). For some sources not in the first two lists, the two-frequency catalog of Pauliny-Toth, Wade, and Heeschen (1966) permitted L_R to be estimated by using equations (3) and (6).

For Parkes sources, L_R was calculated by adopting the listed value of n from the relevant sections of the Parkes catalog and using equations (3) and (6). For the remaining sources with no detailed spectral information, a value of $n = 0.7$ was assumed which, together with a measured flux at one frequency, permits the calculation. Additional quasars not contained in table 3 but for which redshifts and radio data exist are listed in table 4.

Figure 7 illustrates several points, some of which have been discussed elsewhere (Sandage 1966*c*).

TABLE 4

ADDITIONAL RADIO QSOs NOT LISTED IN TABLE 3

Source	Other	z	$m - M$	log L_R, $H = 50$
		3C		
205	...	1.534	44.81	45.22
311	4C 60.19	1.022	43.93	44.68
407	...	1.864	45.24	45.17
		4C		
5.34	...	2.877	46.18	45.03
17.46	...	1.449	44.69	44.64
19.31	...	1.691	45.03	44.65
21.38	...	1.557	44.85	44.48
25.05	...	2.358	45.75	44.86
25.40	...	0.268	41.03	43.03
33.03	...	1.455	44.70	44.74
37.43	...	0.370	41.73	43.65
42.01	5C 3.20	1.588	44.89	44.45
48.28	...	0.385	41.81	43.44
49.22	...	0.334	41.50	43.64
55.27	...	0.249	40.87	43.05
		5C		
2.10	...	0.478	42.28	42.33
2.56	...	2.388	45.78	44.54
		PKS		
0115+02	4C 2.4	0.672	43.02	44.28
0155−10	...	0.616	42.83	44.35
0214+10	...	0.408	41.94	43.77
0424−13	...	2.165	45.56	44.90
0932+02	...	0.659	42.98	44.15
1004+13	4C 13.41	0.240	40.79	43.36
1055+20	4C 20.24	1.11	44.11	44.88
1317−00	4C−0.50	0.89	43.63	44.58
1634+26	3C 342	0.561	42.63	44.11
1801+01	...	1.522	44.80	45.10
2128−12	...	0.501	42.38	44.03
2144−17	...	0.684	43.06	44.37
		PKS Ext (J. V. Wall)		
0225−014	...	0.685	43.06	43.78
0231+022	...	0.322	41.42	42.52
0922+005	...	1.72	45.06	44.88
1335+023	...	0.61	42.81	43.21
2134+004	...	1.936	45.32	(45.2)
2153−204	...	1.31	44.47	44.16
2254+024	...	2.09	45.49	44.87

a) Radio galaxies (*dots*) reach as high a luminosity L_R as do quasars. Cygnus A and Her A at $\log L_R \simeq 45.3$ are nearly as bright as the brightest radio quasar (3C 298) which has $\log L_R \simeq 45.6$.

b) There appears to be an upper limit to the radio power at $\log L_R \simeq 45.6$ ($L_R \simeq 4 \times 10^{45}$ ergs s^{-1}). This is shown by a dashed horizontal line.

c) The apparent increase in L_R with z is a selection effect only, caused by catalog limits to the apparent flux. The sloping lines are loci of constant apparent flux densities at 178 MHz for sources with assumed index $n = 0.7$. (These lines curve slightly at high redshifts due to the K-correction of equation [4].) Lines of 10, 3, and 1 flux units are shown.

d) The vertical line at $z = 2.8$ is a boundary, to the right of which no sources exist in the present sample. The line intersects the upper envelope line near the limit of the 3C catalog at 10 f.u., which illustrates the effect mentioned earlier that sources in the 3C cannot have larger z values than $z \simeq 2.6$ because of this selection.

However, we *would* expect to find larger redshifts for quasars identified from the deeper 4C, 5C, PKS, and Bologna catalogs. The limit of these catalogs are: 9 f.u. at 178 MHz for 3C; 2 f.u. at 178 MHz for 4C; 0.0115 f.u. at 408 MHz for 5C, which corresponds to $\simeq$0.026 f.u. at 178 MHz if $n = 0.7$; 4 f.u. at 400 MHz for PKS, which would be 7.1 f.u. at 178 MHz if $n = 0.7$; and 0.2 f.u. at 408 MHz for the Bologna B2 catalog, or 0.36 f.u. at 178 MHz transformed with $n = 0.7$.

The triangular area between the $l = 3$, the $z = 2.8$, and the $\log L_R = 45.6$ lines should not, therefore, be denied to observers using the 4C, 5C, or Bologna catalogs as source lists. The fact that this area is empty shows that either (1) not enough 4C

sources have yet been observed for their absence in that area to be statistically significant or (2) no larger redshifts do, in fact, exist, because otherwise we would expect quasars with $z \simeq 8$ to be present in those catalogs whose lower limits is 3 f.u. (178 MHz).

Conclusion.—The upper boundary to z in figure 6 is not caused by the radio selection effect related to the natural upper limit to absolute radio power when using catalogs with fixed lower limits to apparent radio flux.

There may, however, be another selection effect from the optical side.

2. To the extent that observers select (for redshift determination) only those quasar candidates that have an ultraviolet excess, high-z quasars could be lost from both the radio and the radio-quiet samples if the excess disappears at high redshift. Figure 8 shows the measured $U - B$ values for all quasars in tables 3 and A1 of the Appendix, plotted against redshift. The well-known semisystematic variation for $z < 2.2$ is shown. The quasars with the two highest redshifts in the present sample are added to the plot at $U - B = -0.28$ for PHL 957, and $U - B = -0.04$ for 4C 5.34.

That the $U - B$ excess might die at large redshifts had been suspected from the time the systematic variation of color with z was understood: the first explicit statement was that by Bahcall and Sargent (1967). Calculations were given by Grewing (1967), and later by Grewing and Lamla (1968), from which the solid curve for $z < 2.2$ is taken as shown in figure 8. The expected color variation for $z > 2.2$ is uncertain because the "average" quasar continuum is unknown below $\lambda_0 \simeq 1000$ Å. We have dotted a *possible* relation in figure 8 for this interval based solely on the two observed objects. There is no assurance that this represents the mean relation for all high-z quasars. This can be known only when more data become available. Nevertheless, figure 8 does suggest that quasars with $z > 2.5$ may have $U - B$ colors that would imitate the colors of F subdwarfs ($U - B \simeq -0.25$) more closely than low-redshifted quasars (i.e., $U - B$ bluer than ~ -0.5 mag).

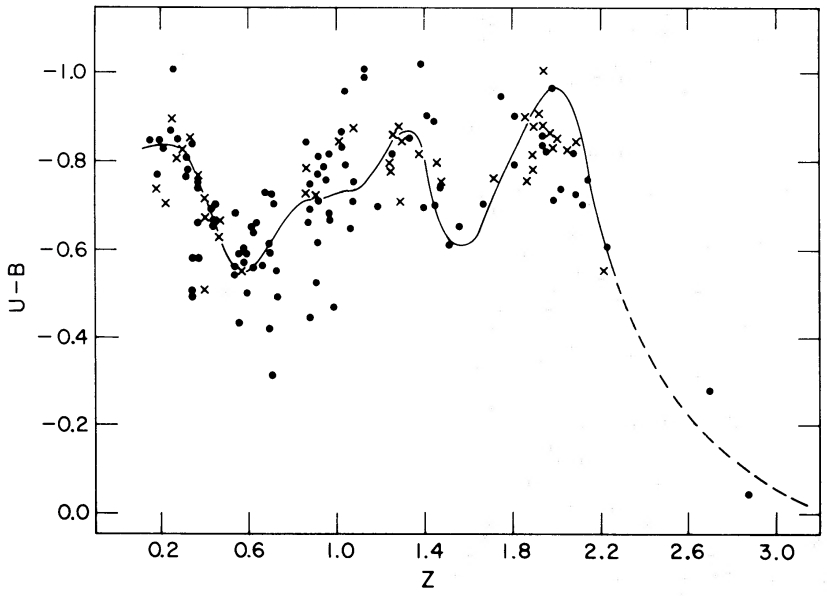

FIG. 8.—$U - B$ color versus redshift for quasars from table 3. *Dots*, radio sources; *crosses*, radio-quiet quasars. The solid line shortward of $z = 2.2$ is from the calculations of Grewing and Lamla. The dotted extension for $z > 2.2$ is schematic and may not apply to all sources.

The vertical crosses in figure 6 are radio-quiet quasars, chosen initially because of their $U - B$ excess. The selection effect of figure 8 could then clearly produce the boundary in figure 6 for these optically identified quasars.

However, this selection effect *need* not occur for radio quasars that are identified on the basis of radio and optical positional coincidence alone. Only to the extent that observers for redshift have chosen such radio candidates which are themselves blue in $U - B$ would there be a color selection for the *triangles* in figure 6. If no such bias exists, the cutoff could not be due to this cause. But it is not certain how strictly this color-blind proviso has been adhered to in the redshift lists at this writing, and our conclusion must remain tentative.

Two observational programs then suggest themselves to test if optical bias has caused the redshift cutoff in figure 6.

A) Spectra of *all* candidates for radio-source identifications from the 4C, 5C, and Bologna (cf. Grueff and Vigotti 1972) catalogs should be obtained, not only those with decidedly blue optical colors.

B) Spectra should be obtained for radio-quiet candidates that lie in the subdwarf region of the $(U - B, B - V)$-diagram of search lists (cf. Sandage and Luyten 1969, fig. 1, hereafter called SL).

Some progress toward these goals has been made. (1) Spectra of several red candidates for quasar identifications in the work of Grueff and Vigotti (1972) show them to be stars. (2) After the surprise (Lowrance *et al.* 1972) concerning the nature of PHL 957 which has subdwarf colors, Schmidt obtained spectra of a number of similar candidates that also have subdwarf colors in the SL survey fields, and all turned out to be stars.

Neither of these tests is definitive in that it cannot be said with certainty that the redshift cutoff at $z \simeq 2.8$ in figures 6 and 7 is real; but neither has it been established that there are selection effects that have caused it artificially. A principal conclusion of this paper is that although the crucial observations have not yet been made, they are straightforward, though tedious, and can be done with existing equipment.

b) Significance of the Cutoff if Real

The redshift cutoff concerns the time into the past before luminous quasars existed. The look-back proper time for objects with $z = 3$ is 89 percent of the creation (Friedmann) time, if $q_0 = +1$ (cf. table 2 of Sandage 1961). Hence, light left quasars with that redshift at a time $0.11t_0$ away from the emergence of the Universe out of the Friedmann singularity. Upon looking further out into space, and hence back to earlier epochs in time, we presumably would fail to see quasars because they had not yet been born.

Such a redshift cutoff must, of course, occur at some large but finite redshift in all evolutionary cosmologies because galaxies have not always existed but began their birth at a particular epoch. It is at first surprising that the critical epoch when quasars first turned on might be at a redshift as small as 3 rather than $z \simeq 1000$. However, there must be a collapse time between the beginning of the decoupling of matter from radiation in the early Universe and the time when the galaxies (or quasars) began to shine. If this time is $\sim 10^9$ years, then $z \simeq 3$ is the appropriate horizon redshift.

But arguments such as these are seldom secure, and the next step must be a critical observational study to test the reality of the cutoff. The possibility that we have already seen to the edge of the world is quite remarkable. To prove that we have would be quite unique.

The observational data upon which this paper is based have been obtained since 1964 with the efficient help of the night assistants Gary Tuton and Juan Carrasco on Palomar, and Eugene Hancock and Al Olmstead on Mount Wilson. The pulse-count-

ing and data systems of the Astroelectronics Laboratory were used in the later stages of the work on both mountains.

It is a pleasure to thank the Australian-American Educational Foundation for a fellowship in Australia, Professor O. J. Eggen for the hospitality of the Mount Stromlo Observatory of the Australian National University where this paper was written, and Jerome Kristian for reading and commenting on a draft of the manuscript.

APPENDIX

Table A1 lists *UBV* photometry of quasars which were measured in the identification program during 1966 and 1967 which have not been published. The observations were made with the 200-inch reflector in the same way as the bulk of the observations in table 3. The errors are expected to be smaller than ± 0.05 (rms) mag for all listed colors and magnitudes.

TABLE A1

PHOTOMETRY OF QSO CANDIDATES NOT PREVIOUSLY REPORTED

Object	V	$B-V$	$U-B$	Date	Object	V	$B-V$	$U-B$	Date
3C 39	18.09	+0.31	−0.59	11/2/67	0122−00	16.70	+0.28	−0.75	10/2/67
205	17.62	+0.48	−0.48	9/2/67	0229+13	17.71	+0.25	−0.73	10/2/67
323.1	16.69	+0.11	−0.85	20/6/66	0350−07	16.49	+0.44	−0.68	10/2/67
					0403−13	17.09	+0.28	−0.57	10/2/67
4C−05.93*	17.70	+0.75	−0.71	11/8/67	0736+01	16.47	+0.43	−0.77	9/2/67
20.33	17.65	+0.44	−0.69	20/6/66	0859−14	16.59	+0.20	−0.85	9/2/67
21.35	17.50	+0.06	−0.69	20/6/66	0952+17	17.23	+0.08	−0.74	9/2/67
29.50	19.14	+0.15	−0.86	20/6/66	1354+19	16.03	+0.30	−0.62	20/6/66
29.68	17.30	+0.65	−0.87	21/6/66	1454−06	18.03	+0.36	−0.82	9/2/67
31.38	18.96	+0.37	−0.65	20/6/66	2216−03	16.38	+0.55	−0.62	21/6/66
37.24	18.11	+0.42	−0.81	9/2/67	2354+14	18.18	+0.14	−0.90	20/6/66
39.25	17.86	+0.06	−0.31	9/2/67					

* PHL 5200.

REFERENCES

Arp, H. C. 1970, *Ap. Letters*, **5**, 257.
———. 1971, *ibid.*, **9**, 1.
Bahcall, J. N., and Sargent, W. L. W. 1967, *Ap. J. (Letters)*, **148**, L65.
Bennett, A. S. 1962, *Mem. R.A.S.*, **68**, 163.
Bolton, J. 1960, *Obs. Owens Valley Obs.*, No. 5.
Burbidge, E. M. 1967, *Ap. J. (Letters)*, **149**, L51.
Greenstein, J. L. 1961, *Ap. J.*, **133**, 335.
———. 1962, *ibid.*, **135**, 679.
Grewing, M. 1967, *Zs. f. Ap.*, **67**, 283.
Grewing, M., and Lamla, E. 1968, *Zs. f. Ap.*, **68**, 473.
Griffin, R. F. 1963, *A.J.*, **68**, 421.
Grueff, G., and Vignotti, M. 1972, *Astr. and Ap. Suppl.*, **6**, 1.
Gunn, J. E. 1971, *Ap. J. (Letters)*, **164**, L113.
Hazard, C. 1965, *Quasi-stellar Sources and Gravitational Collapse, ed. I. Robinson*, A. E. Schild, and E. L. Schucking (Chicago: University of Chicago Press), p. 135.
Heeschen, D. S. 1966, *Ap. J.*, **146**, 517.
Hogg, D. E. 1969, *Ap. J.*, **155**, 1099.
Hoyle, F., and Burbidge, G. R. 1966, *Nature*, **210**, 1346.
Howard, W. E., Dennis, T. R., Maran, S. P., and Aller, H. D. 1965, *Ap. J. Suppl.*, **10**, 331.
Humason, M. L., Mayall, N. U., and Sandage, A. 1956, *A.J.*, **61**, 97.
Kellermann, K. I. 1964, *Ap. J.*, **140**, 969.

Kinman, T. D. 1968, *A.J.*, **73**, 885; pl. S-VIII (p. 927).
Kristian, J. 1972, *Ap. J.* (*Letters*) (in preparation).
Legg, T. H. 1970, *Nature*, **226**, 65.
Longair, M. S. 1965, *M.N.R.A.S.*, **129**, 419.
Longair, M. S., and Scheuer, P. A. G. 1967, *Nature*, **215**, 919.
Lowrance, J. L., Morton, D. C., Zucchino, P., Oke, J. B., and Schmidt, M. 1972, *Ap. J.*, **171**, 233.
Lynds, C. R., and Millikan, A. G. 1972, *Ap. J.* (*Letters*), **176**, L5.
Mackay, C. D. 1971, *M.N.R.A.S.*, **154**, 209.
Maltby, P., Matthews, T. A., Moffet, A. T. 1963, *Ap. J.*, **137**, 153.
Matthews, T. A., Morgan, W. W., and Schmidt, M. 1964, *Ap. J.*, **140**, 35.
Matthews, T. A., and Sandage, A. 1963, *Ap. J.*, **138**, 30.
Miley, G. K. 1971, *M.N.R.A.S.*, **152**, 477.
Minkowski, R. 1960, *Ap. J.*, **132**, 908.
———. 1961, *A.J.*, **66**, 558.
Pauliny-Toth, I. I. K., Wade, C. M., and Heeschen, D. S. 1966, *Ap. J. Suppl.*, **13**, 65.
Rogstad, D. H., and Ekers, R. D. 1969, *Ap. J.*, **157**, 481.
Ryle, M. 1968, in *Highlights of Astronomy*, ed. L. Perek (Dordrecht: D. Reidel Publishing Co.), p. 33.
Sandage, A. 1961, *Ap. J.*, **134**, 916.
———. 1966*a*, *ibid.*, **145**, 1.
———. 1966*b*, *ibid.*, **146**, 13.
———. 1966*c*, in *High Energy Astrophysics of the International School of Physics* "Enrico Fermi," Course 26 (New York: Academy Press), p. 33.
———. 1967*a*, *Ap. J.* (*Letters*), **150**, L9.
———. 1967*b*, *ibid.*, p. L145.
———. 1967*c*, *ibid.*, p. L177.
———. 1971, *Optical Properties of Nuclei, in Semaine d'Etude sur Les Noyaux des Galaxies* (Pont. Acad. Sci. Scripta Varia No. 35), ed. D. O'Connell, p. 271.
———. 1972*a*, *Ap. J.*, **173**, 485 (Paper I).
———. 1972*b*, *ibid.*, **178**, 1 (Paper II).
Schmidt, M. 1965, *Ap. J.*, **141**, 1.
Wyndham, J. W. 1965, *A.J.*, **70**, 384.
———. 1966, *Ap. J.*, **144**, 459.
Zwicky, F., and Humason, M. L. 1964, *Ap. J.*, **139**, 296.